Case Reports in Ophthalmology

Case Rep Ophthalmol 2021;12:749–760
DOI: 10.1159/000512284
Received: July 2, 2020
Accepted: October 10, 2020
Published online: September 9, 2021

Case Report

Two Novel Disease-Causing Variants in the PDE6C Gene Underlying Achromatopsia

Carolina Madeira[a] Gonçalo Godinho[a] Ana Grangeia[b] Manuel Falcão[a, c] Renato Silva[a, c] Ângela Carneiro[a, c] Elisete Brandão[a] Augusto Magalhães[a] Fernando Falcão-Reis[a, c] Sérgio Estrela-Silva[a, c]

[a]Department of Ophthalmology, Centro Hospitalar e Universitário de São João Hospital, Porto, Portugal; [b]Department of Genetics, Centro Hospitalar e Universitário de São João Hospital, Porto, Portugal; [c]Department of Surgery and Physiology, Faculty of Medicine of University of Porto, Porto, Portugal

Keywords
PDE6C gene · Achromatopsia · Multimodal imaging

Abstract
We report the clinical phenotype and genetic findings of two variants in PDE6C underlying achromatopsia (ACHM). Four patients with the variant c.1670G>A in exon 13 of the PDE6C gene were identified. Additionally, one had compound heterozygous genotype, with two variants in the *PDE6C* gene, a variant of c.2192G>A in exon 18 and c.1670G>A in exon 13. All patients presented the symptomatic triad of decreased visual acuity, severe photophobia, and colour vision disturbances. SD-OCT showed an absence of the ellipsoid zone, creating an optically empty cavity at the fovea in three patients. The patient with the compound heterozygous genotype presented a more severe subfoveal outer retina atrophy. ERG recordings showed extinguished responses under photopic and 30-Hz flicker stimulation, with a normal rod response. We identified two new variants in the *PDE6C* gene that leads to ACHM.

Introduction

Achromatopsia (ACHM) is a rare disorder with a frequency of 1:30,000 to worldwide [1]. ACHM is characterized by birth or early infancy poor visual acuity (VA), pendular nystagmus, photophobia and reduced or absent colour vision loss along all 3 axes [2–4]. This condition is inherited in an autosomal recessive pattern [5, 6]. However, genotype-phenotype correlations

Correspondence to:
Sérgio Estrela-Silva, sestrelasilva@gmail.com

are often difficult to establish, because pathogenic variants in different genes can cause similar phenotypes and pathogenic variants in the same genes can cause a broad-spectrum of phenotypes [7, 8].

Cyclic-nucleotide phosphodiesterases of the sixth family (*PDE6*) have a key role in phototransduction cascade [9]. In rods, this enzyme is a heterodimer of *PDE6A* and *PDE6B* subunits and in cones it is a homodimer of *PDE6C* subunits [10].

The *PDE6C* gene encodes the cone α subunit of cyclic guanosine monophosphate (cGMP) phosphodiesterase [10, 11]. During light exposure the photopigment is excited and, via guanosine diphosphate (GDP)/guanosine-5′-triphosphate (GTP) exchange and release of the Ga-subunit, activates the G-protein transducing. Ga-subunit binds and displaces the *PDE6* inhibitory g-subunit, activating the catalytic *PDE6* dimer. The later, rapidly hydrolyzes intracellular cGMP molecules, allowing the closure of cGMP-gated ion channel in the cone outer segment membrane, leading to hyperpolarization.

Loss or dysfunction of any component of the phototransduction cascade results in photoreceptor degeneration and significant visual function loss [11]. Pathogenic variants in the PDE6C gene are phenotypically related to CD and ACHM [3, 12–15]. The PDE6C genotype in ACHM patients is rare and it has an estimated prevalence of 2.4% in a cohort of 1,074 independent ACHM families [14]. The purpose of this study is to report the clinical phenotype and genetic findings of two novel disease-causing variants in the *PDE6C* gene underlying ACHM.

Case Report

Methods

Patients

We describe the clinical and genetic screening findings from four patients in a single tertiary centre from Portugal, Centro Hospitalar e Universitário de São João. This was a retrospective observational study and it was conducted in accordance with Declaration of Helsinki and local Ethics Committee approval was obtained. A written informed consent was given to all participants or to their legal guardians.

Patients 1 and 2 were siblings. The other 2 patients were unrelated. A pedigree of each case was assembled based on a detailed family history with regards to ocular diseases and visual symptoms.

Clinical Investigations

The medical chart of the patients were reviewed. Full ophthalmological examination has been performed, including best-corrected Snellen visual acuity (VA) assessment, slit-lamp biomicroscopy and detailed fundus examination.

Colour vision was evaluated using the Farnsworth-Munsell 100 Hue Test. Additionally, Ishihara colour test was performed under standard conditions in patients 3 and 4. Fundus colour photography were taken using the VISUCAMPRO NM from ZEISS. All patients underwent a standardized retinal imaging, including spectral-domain optical coherence tomography (SD-OCT), fundus autofluorescence (FAF) and fluorescein angiography (FA). These images were obtained using the SD-OCT System Heidelberg Engineering, Heidelberg, Germany. Central foveal thickness was manually measured as the distance between the vitreoretinal interface and the posterior edge of the retinal pigment epithelium at the umbo.

Electrophysiological evaluation included full-field electroretinograms (ERGs) using a Ganzfeld dome and pattern ERG. The ERG testing was performed according to the protocol of the International Society for Clinical Electrophysiology of Vision [16]. All the electrophysiological

exams were performed using a Metrovision system. Patients undergone visual field testing with goldmann kinetic perimetry, performed by a trained orthoptist.

Molecular Genetic Analysis

DNA was isolated from peripheral blood leukocytes using the conventional salting-out procedure. Healthy parents from patients 1 and 2 also underwent genetic analysis.

Targeted genetic analysis was performed using a combination of next-generation sequencing panel and Sanger sequencing. Details of panel design, library preparation, and capture sequencing has already been published [17]. The panel include 29 genes associated with cone-rod dystrophy. The full coding region and nearly 20 nucleotides of flaking non-coding intronic DNA of the 29 genes were sequenced. Sanger sequencing was performed for any regions not captured or with insufficient number of sequences reads. All pathogenic and undocumented variants were confirmed by Sanger sequencing.

Results

Clinical features and identified genotypes of the four patients are summarized in Table 1. Patients 1 and 2 were siblings, and the other 2 were unrelated. All patients described had no family history of cone dystrophy.

Patients 1 and 2

Patients 1 and 2 are siblings with a current age of 28 and 29 years old, respectively. The pedigree is presented in Figure 1. Both patients have been followed in our department since childhood. Both presented binocular rotatory nystagmus in all gaze position, without a null point in the first decade of life. However, patient 1 had a binocular 40 prism diopter esotropia and cross-fixation and in patient 2 no strabismus were observed. The anterior segments and fundoscopy were within normal limits.

Both had similar VA and a myopic refractive error. Patient 1, at the age of 4, and patient 2, at the age of 6, had a best-corrected VA of, respectively, 20/100 in both eyes (OU) and 20/200 in OU. Over the years, these patients maintained a poor VA, presenting both a current BCVA of 20/200 in OU. At the end of follow-up, the patients presented a myopic refractive error, higher in patient 2.

The siblings never complained of night blindness and peripheral vision loss, but they had moderate photophobia. Patients recall colour vision discrimination in the early childhood, with subsequent progressive worsening. Ocular fundus examination was unremarkable.

They underwent multimodal imaging (Fig. 2, 3). In patient 1, SD-OCT showed an absence of the ellipsoid zone and of the photoreceptor outer segments, creating a subfoveal optical empty cavity. Despite without a greater extension, this subfoveal optic empty cavity was also observed in patient 2 OS. Instead in the OD, a granular appearance of the ellipsoid zone was present. In both cases, the central subfoveal (CSF) thickness was reduced, particularly in patient 2. CSF in patient 1 was 110 and 117 μm in the right eye (OD) and the left eye (OS), respectively, whereas, in patient 2, CSF was 88 and 87 μm in the OD and OS, respectively. The FAF revealed mild perifoveal hyperautofluorescent ring in OU of both patients. Only patient 1 performed FA and an early diffuse mottled hyperfluorescence was perceptible in this exam.

Goldman kinetic visual field testing in patient 1 gave normal results and in patient 2 showed a discrete peripheral constriction (Fig. 3). The siblings underwent colour vision testing with Farnsworth-Munsell 100 Hue Test, revealing multiple errors in all 3 axes.

In the case of patient 1, electroretinography was performed at the ages of 10 and 11, respectively. In the initial recordings, dark-adapted (DA) 0.01 ERG and DA 3 ERG were

Table 1. Clinical ocular features in the patients

Clinical feature	Patient 1	Patient 2	Patient 3	Patient 4
Age of onset, years	3 months	?	7 months	3 months
Visual complaints				
Photophobia	Yes	Yes	Yes	Yes
Nystagmus	Yes	Yes	Yes	Yes
Nictalogia	No	No	No	No
Peripheral visual loss	No	No	No	No
Strabismus	Yes, ET	No	Yes, XT	Yes, XT
Initial refractive error	OD +1.50 OS +1.75	OD -2.00 -2.00 × 15° OS -2.75 -2.00 × 160°	?	OD + 1.25 × 95 OS + 1.25 × 85
First BCVA, years	4	6	?	4
First BCVA (Snellen)	20/100	20/200	?	20/50
Age final, years	29	28	30	11
Final BCVA (Snellen)	20/200	20/200	20/200	20/200
Final refractive error	OD -0.75-0.5 × 20° OS -1.25 × 110°	OD -6.50-2.00 × 25° OS -6.00-2.00 × 170°	OD -5.00-1.75 × 70° OS -7.00-2.00 × 140°	OD +1.00 + 1.00 × 90° OS +1.75 + 1.25 × 70°
Color discrimination	Impairment in the three colour axes	Impairment in the three colour axes	Impairment in the three colour axes	Impairment in the three colour axes
Ocular Fundus	Normal	Normal	OD macular atrophy OS "bull's eye" maculopathy	Normal
ffERG final	Normal DA LA 3 ERG and LA 30-Hz flicker ERG severely reduced and delayed	Normal DA LA unrecordable	Normal DA LA 3 ERG and LA 30-Hz flicker ERG severely reduced and delayed	Normal DA LA unrecordable
SD-OCT	OU Disruption of ellipsoid and photoreceptor outer segment	OD Ellipsoid irregularity OS Disruption of ellipsoid and photoreceptor outer segment	OD atrophy of external layers of retina OS Disruption of ellipsoid and photoreceptor outer segment	?
FAF	Mild perifoveal hyperautofluorescent ring in OU	Mild perifoveal hyperautofluorescent ring in OU	OD complete loss of normal macular autofluorescence OS increase of hypoautofluorescence	?

ET, esotropia; XT, exotropia; OD, oculus dextrus; OS, oculus sinistre; ERG, electroretinogram; DA, dark-adapted; LA, light-adapted; SD-OCT, spectral-domain optical coherence tomography; FAF, fundus autofluorescence.

Case Rep Ophthalmol 2021;12:749–760
DOI: 10.1159/000512284

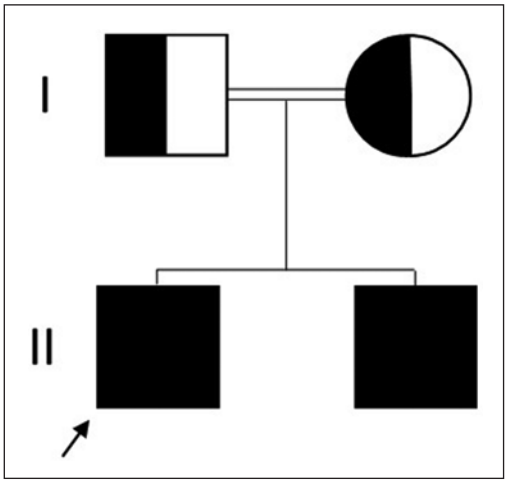

Fig. 1. Patients 1 and 2 family pedigree. Squares represent males and circles represent females. Filled symbols represent affected individuals. The proband is marked with an arrow.

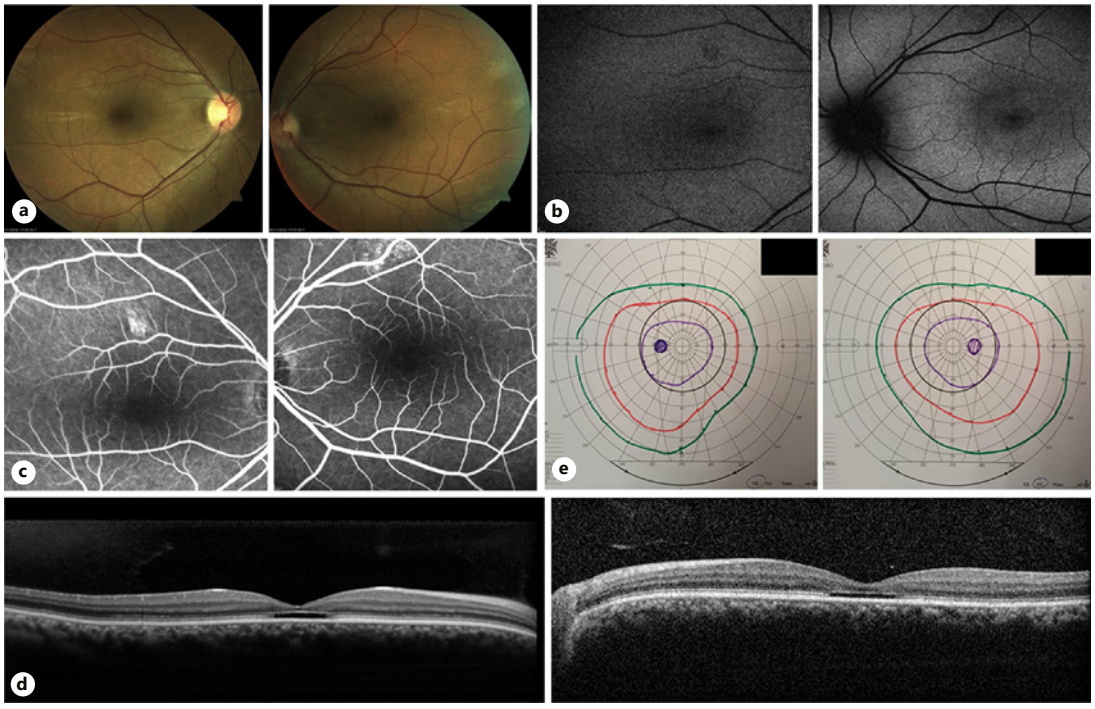

Fig. 2. Clinical phenotype of patient 1. **a** Fundus image was entirely normal. **b** FAF showed an hyperautoflurescence ring at the perifoveal region in both eyes. **c** On FA early diffuse mottled early hyperfluorescence was perceptible. **d** SD-OCT revealed an absence of the ellipsoid zone and of the photoreceptor outer segments, creating a subfoveal optical empty cavity. **e** Goldmann kinetic perimetry testing was normal. FAF, fundus autofluorescence; FA, fluorescein angiography; SD-OCT, spectral-domain optical coherence tomography.

normal, and light-adapted (LA) 3 ERG and LA 30-Hz flicker ERG were subnormal. Pattern ERG was normal. In the full-field ERG performed 2 years later, the amplitude of the DA 0.01 and DA 3 ERG was normal. The LA 3 ERG and LA 30-Hz flicker ERG were severely reduced and delayed. The P50 wave on the pattern ERG was undetectable. In patient 2, the ERG full-field performed at the age of 11 years old displayed a normal DA ERG responses and nonrecordable LA ERG responses. Pattern ERG showed a reduction of the P50 wave. In both cases,

Case Rep Ophthalmol 2021;12:749–760
DOI: 10.1159/000512284

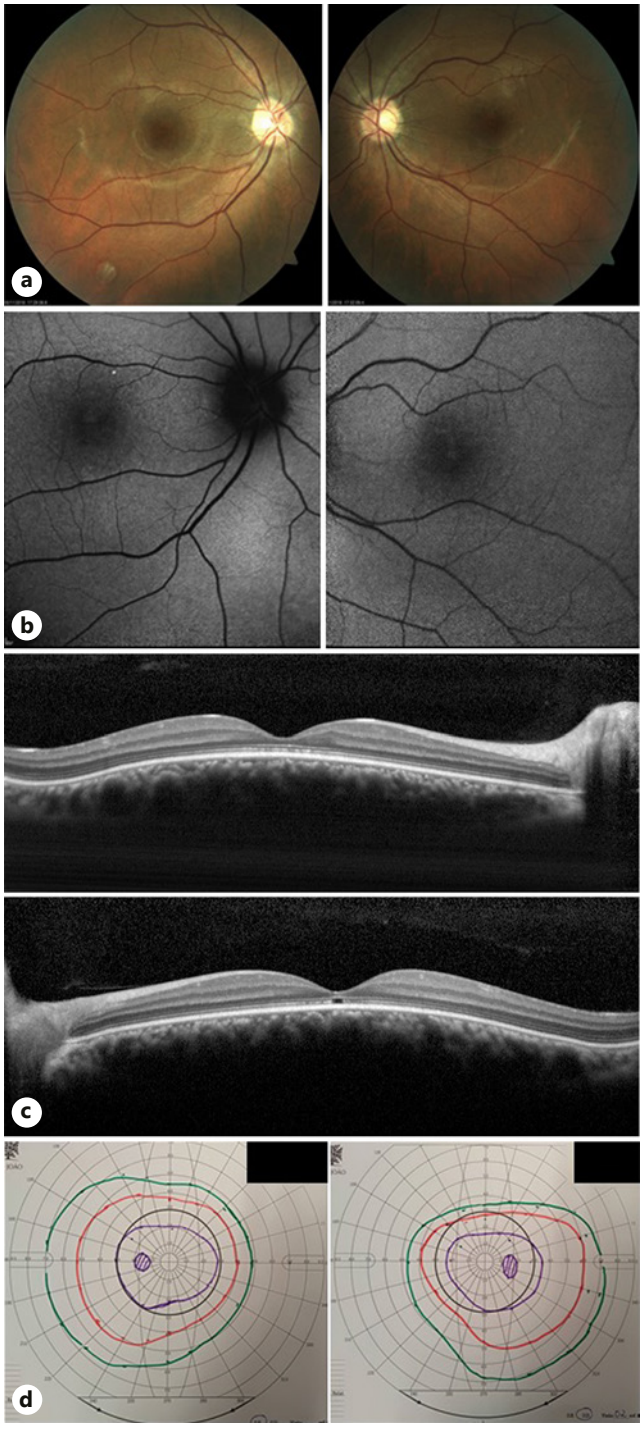

Fig. 3. Clinical phenotype of patient 2. **a** Fundus image was unremarkable. **b** FAF showed an hyperautoflurescence ring at the perifoveal region in both eyes. **c** SD-OCT disclosed a granular appearance of ellipsoid in the OD and a disruption of the subfoveal ellipsoid and photoreceptors outer segments in the OS, creating an optical empty cavity. **d** Goldmann kinetic perimetry testing showing a discrete peripheral constriction. FAF, fundus autofluorescence; OD, right eye; OS, left eye; SD-OCT, spectral-domain optical coherence tomography.

the results of electrophysiology testing were consistent with cone dysfunction with macular impairment.

Patient 3

Patient 3 was a 30-year-old Brazilian male whose parents were Portuguese, without a family history of consanguinity or ophthalmological disorders. He was first observed at our centre at the age of twenty-nine. He presented a history of nystagmus since he was 7 months old.

Symptoms of photophobia were present at an early age. He did not complain of night blindness and peripheral vision loss. Best-corrected VA was 20/200 in OU. He presented refractive error of −6.00 and −8.00 dioptres in the OD and OS, respectively. He had a 15 prism dioptre binocular exotropia.

The anterior segments were normal. The fundus showed a macular atrophy in the OD and a mild macular RPE changes in a "bull's eye" pattern in the OS. Optic disc, retinal vessels, and peripheral retina were normal (Fig. 4).

FAF demonstrated a small, round, hypoautofluorescent macular lesion in the OD and a discrete hyperautofluorescent ring at the perifoveal region in OS. SD-OCT scans revealed in the OD an atrophy of both inner and outer subfoveal retina, with well-limited borders. The OS showed an atrophy of photoreceptor external segments. There was reduced retinal thickness at the fovea, with a mean CSF thickness 32 μm for the OD and 74 μm for the OS. FA demonstrated an early diffuse hyperfluorescent mottling in OU and in the OD a macular hyperfluorescence due to a window defect.

Goldman kinetic perimetry revealed a normal visual field. Farnsworth-Munsell 100 Hue Test results showed multiple errors in all 3 axes.

Also, an Ishihara colour test was performed. The patient recognized plates number 1 and 6–8 and partially plates 3 and 9 plates (such as patients with red-green deficiencies).

Electrophysiological test (Fig. 5) performed by the age of 30 and revealed a normal DA 0.01 ERG and DA 3 ERG responses. The LA 3 ERG was unrecordable and LA 30-Hz flicker ERG was severely delayed. On pattern ERG P50 wave was undetectable. These results were compatible with cone system dysfunction associated with macular impairment.

Patient 4

Patient 4 is an 11-year-old boy that presented pendular nystagmus and intense photophobia since he was 3 months. His medical history was unremarkable, and there was no family history of serious ophthalmologic diseases or consanguinity.

At the age of 5, he presented a best-corrected VA of 20/50 bilaterally. He had a low hypermetropic refractive error (+1.00 and +1.50 in OD and OS, respectively). Examination showed a 5 prism diopter exotropia of the OS. Ocular fundus examination was entirely normal.

Over time VA decreased. Currently, he is 11 year old and his best-corrected VA is 20/200 in OU. The first electrophysiological test performed at the age of 3 revealed DA adapted ERGs within normal limits, but the LA 3.0 ERG and LA 30-Hz flicker ERG were nonrecordable (Fig. 5). These results indicated a cone dysfunction and normal rod function.

Colour vision was tested. Farnsworth-Munsell 100 Hue Test presented multiple errors is the 3 axes. Additionally, colour vision was tested using Ishihara colour plates in standard conditions. The boy recognized plates number 1 and 14 and partially plates 5 and 7–8 plates (such as patients with red-green deficiencies).

Fundus colour photography, SD-OCT, FA, and FAF are not displayed, was unable to cooperate to perform these exams due to the intense photophobia, nystagmus, and the young age.

Genetic Analysis

Table 2 shows a summary of the molecular results of all patients. Patient number 1 and 2 were diagnosed with ACHM. The genetic analysis using a next-generation sequencing panel for cone dystrophy/ACHM screening identified the variant c.1670G>A in homozygosity in the exon 13 of *PDE6C* gene in both patients. This missense variant results in the substitution of the arginine residue in the codon 557 by glutamine, which change resides within the protein domain (3′5′ cyclic-nucleotide phosphodiesterase). The amino acid residue p.Arg557 of the

Case Rep Ophthalmol 2021;12:749–760
DOI: 10.1159/000512284

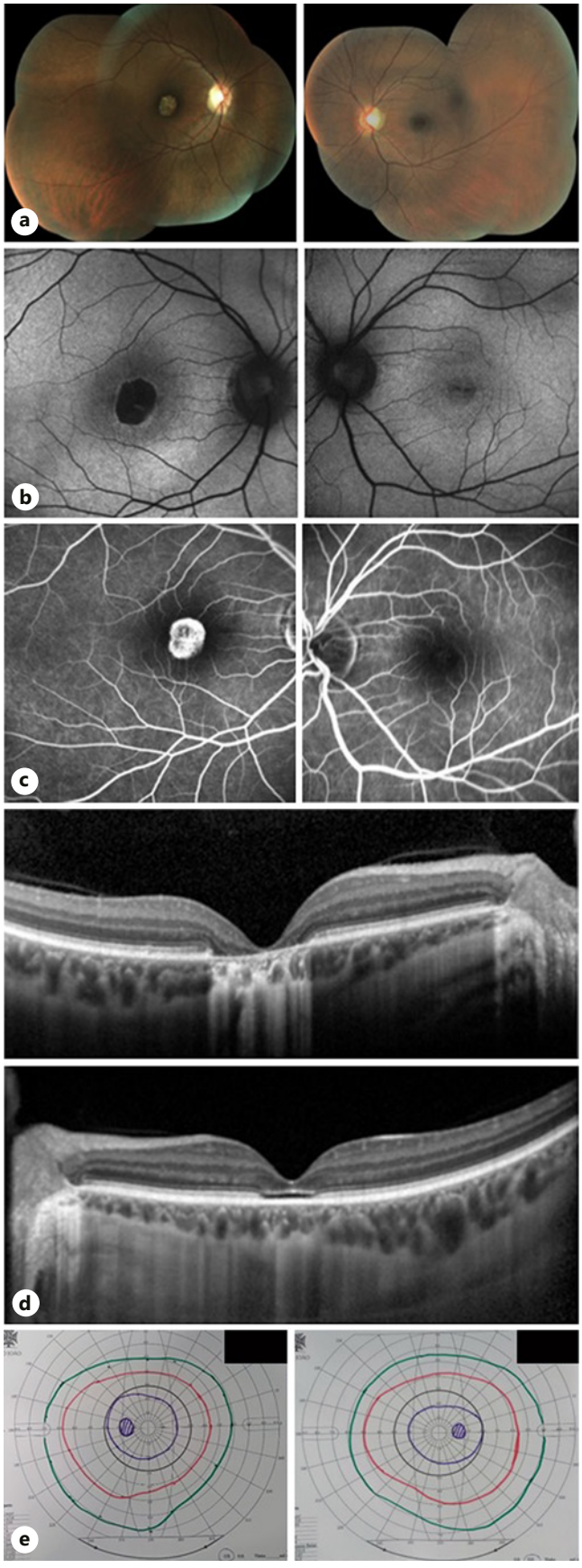

Fig. 4. Clinical phenotype of patient 3. **a** Fundus image showed a macular atrophy in the OD and a mild macular RPE changes in a "bull's eye" pattern in the OS. **b** FAF demonstrated a small, round, hypoautofluorescent macular lesion in the OD and a discrete hyperautofluorescent ring at the perifoveal region in OS. **c** FA showed an early diffuse hyperfluorescent mottling in OU, and in the OD a macular hyperfluorescence due to a widow defect. **d** SD-OCT scans revealed in the OD an atrophy of both inner and outer subfoveal retina, with well-limited borders; and in the OS showed an atrophy of photoreceptors external segments. **e** Goldmann kinetic perimetry testing was normal. OD, right eye; OS, left eye; FAF, fundus autofluorescence; FA, fluorescein angiography; SD-OCT, spectral-domain optical coherence tomography.

Case Rep Ophthalmol 2021;12:749–760
DOI: 10.1159/000512284

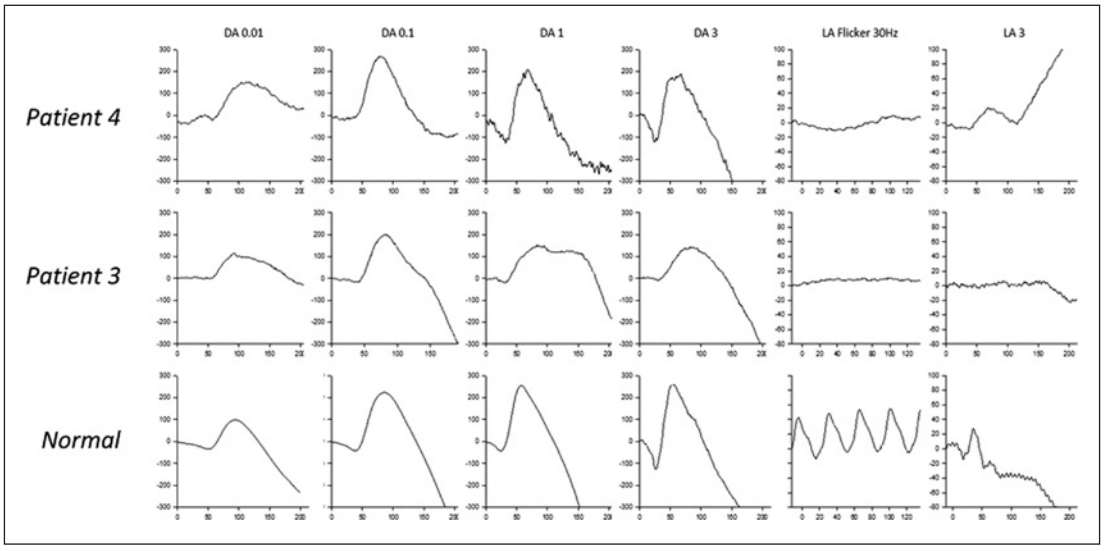

Fig. 5. Full-field ERG acquired on patients 3 and 4. In patient number 4, full-field ERG revealed a nonrecordable LA 3.0 ERG and LA 30-Hz flicker ERG responses. Patient number 3 electrophysiological test showed a normal DA 0.01 ERG and DA 3 ERG responses. The LA 3 ERG was unrecordable, and LA 30-Hz flicker ERG was severely delayed.

Table 2. Genetic molecular findings in the 4 patients studied

	Exon (PDE6C gene)	Nucleotide	Protein effect
Patient 1	Exon 13	c.1670G>A	p.Arg557Gln
	Exon 13	c.1670G>A	p.Arg557Gln
Patient 2	Exon 13	c.1670G>A	p.Arg557Gln
	Exon 13	c.1670G>A	p.Arg557Gln
Patient 3	Exon 13	c.1670G>A	p.Arg557Gln
	Exon 18	c.2192G>A	p.(Trp731Ter)
Patient 4	Exon 13	c.1670G>A	p.Arg557Gln
	Exon 13	c.1670G>A	p.Arg557Gln

PDE6C protein has been highly conserved during evolution. Using the Mutation Taster bioinformatics software, this variant was predicted to be a "disease causing," with a high pathogenicity score for the altered amino acid.

Both unaffected parents were carriers of the c.1670G>A (p.Arg557Gln) variant in heterozygosity in the exon 13 of *PDE6C* gene. There was no history of this disease in the family. Therefore, patients 1 and 2 were isolated cases, which indicates an autosomal recessive mode of inheritance.

Patient 3 had 2 variants in the *PDE6C* gene in compound heterozygosity. A pathogenic variant c.2192G>A (p.[Trp731*]) in heterozygosity in the exon 18 and a pathogenic variant of c.1670G>A in exon 13 of *PDE6C* gene were identified. The variant of c.2192G>A results in a substitution of a tryptophan introducing a premature stop codon, and then originating a truncated protein. Also, according to Mutation Taster bioinformatics software, this new variant was predicted to be a "disease causing," with a high pathogenicity score for the altered amino acid.

Genetic analysis of patient 4 showed a homozygous variant c.1670G>A in exon 13 of *PDE6C* gene. This novel variant, c.1670G>A in exon 13 of *PDE6C* gene, is already described in population based databases, but this is the first time that it is reported as a disease-causing

Case Rep Ophthalmol 2021;12:749–760
DOI: 10.1159/000512284

variant. Additionally, the variant c.2192G>A in exon 18 of *PDE6C* gene identified in patient number 3 is novel and has never been described in the Single Nucleotide Polymorphism Database, the 1,000 Genomes database, the Human Genetic Variation Browser, or the Human Gene Mutation Database.

Discussion

In this study, we report two new *PDE6C* variants causing ACHM. Pathogenic variants in *PDE6C* are predicted to cause loss-of-function of phosphodiesterase, leading to elevation of intracellular cGMP levels and a toxic overload with calcium due to the steady influx of calcium through the cGMP-gated channel [18, 19]. Activation of protein kinase G may also contribute to cGMP-induced death of photoreceptors [18].

Clinical phenotypes of *PDE6C* gene variants range from early onset cone dystrophy to ACHM [12–15]. About 121 different variants in *PDE6C* have been listed on the Human Genome Mutation Database, of those 46 are "pathogenic or likely pathogenic" and 53 are classified as "uncertain significance." To date, *PDE6C* pathogenic variants are responsible for about 2.5% cases of congenital ACHM and 1.8% of cone dystrophies [12, 20, 21]. The variability in clinical phenotypes may be explained by the fact that different variant affects *PDE6C* function differently.

In this study, we report two novels variants in *PDE6C* gene that affected evolutionarily conserved amino acids of a highly conserved region. The variant c.1670G>A in exon 13 occurs in a highly conserved region, in the protein domain 3′5′ cyclic-nucleotide phosphodiesterase, having a severe effect on protein's function. And the variant c.2192G>A in exon 18 of *PDE6C* produces a premature stop codon, originating a truncated protein.

All the reported patients presented nystagmus shortly after birth. The symptoms of our patients included the same triad of decreased VA, severe photophobia, and colour vision disturbances. None of them reported night blindness and peripheral visual loss. The appearance of the ocular fundus was variable. In three cases, it was entirely normal, but one patient presented with macular retinal pigment epithelium atrophy or "bull's eye maculopathy." In previously reported cases of CD associated with PDE6C fundus ocular changes were also subtle, varying from absence of foveal reflex to mild foveal pigmentary changes. Grau et al. [12] also reported one pathogenic variant in PDE6C causing CD. They detected homozygous missense variant in exon 1 (p.Arg29Trp) in both sibling pairs of one non-consanguineous family affecting a conserved residue just upstream of the first GAF (GAF-A) domain [12]. These patients showed an early onset CD; their VA and cone ERG progressively declined in their early teens [12]. The clinical phenotype of their patients was similar to ours. Their patients presented with nystagmus and photophobia and the ocular fundus examination revealed absence of foveal reflex or pigmentary changes.

All of our patients meet the clinical criteria of ACHM. Also, except from patient 4, all patients presented a myopic refractive error. This is in accordance with previous reports, in which majority of the patients with ACHM-PDE6C had high myopia [15].

SD-OCT allows us to study details of foveal microstructure and the disease has been described to go through sequential stages that can be followed on this exam [22]. In our patients, SD-OCT scans showed a disruption of the ellipsoid, outer segment of photoreceptors absence and a decreased thickness of the outer nuclear layer at the fovea in all patients, which is the predominantly cone photoreceptor location. Although these features correlate well with the clinical findings in our study, since in all patients the outer retinal layers of the midperipheral retina were intact, indicating that there was no anatomic rod involvement. Foveal hypoplasia was absent in all patients. Foveal hypoplasia is a common finding of ACHM associated with ATF6, CNGA3, and CNGB3, but not

typical of PDE6C-ACHM [8, 14, 15]. The absence of foveal hypoplasia seems to be a distinctive clinical feature of PDE6C-ACHM.

Patient number 3 presented a compound heterozygous genotype, with two variants in the PDE6C gene, an heterozygotic pathogenic variant of c.2192G>A in exon 18 and a heterozygotic variant c.1670G>A in exon 13. Interestingly, there were some differences between this patient and the others regarding the clinical phenotype. This patient presented with macular atrophy on ocular fundus examination and more severe outer retinal layers atrophy on SD-OCT. We hypothesize that these patients could be in different disease stages or the combination of these two variants may have a more severe effect on the *PDE6C* function, especially because one of the variants originates a truncated protein.

As previously described, none of our patients presented with rod dysfunction in ERG. Even though rod involvement does not appear to be direct a consequence of PDE6C variants, some discrete dysfunction in rods have been described later in life [15, 23]. It seems that PDE6C variants leads to an impairment of S-, M-, and L-cones since ERG cone responses and colour vision are severely affected in these patients.

Recently, there's been some controversy on the stationary or progressive nature of ACHM. In our reported cases, both patients 1 and 2 have about 30 years of follow-up and overtime VA has been relatively stable. However, Georgiou et al. [23] performed a longitudinal study including FAF and OCT of a cohort with PDE6C-associated ACHM and reported a mean annual increase in ellipsoid lesion size of 48.3 μm and a mean hypoautofluorescent area increase of 0.13 mm^2/year. It seems that despite VA remains stable overtime, a slowly progressive maculopathy is present.

In conclusion, we identified two new disease-causing variants in *PDE6C* that leads to ACHM. PDE6C is a potential target for gene therapy, and therefore, it is important to evaluate how the cones are affected by PDE6C sequence variants and better understand the potential of functional rescue. Our data extended the phenotypic spectrum of retinal disorders caused by PDE6C variants and provided new clinical and genetic information.

Ackowledgments

The authors acknowledge the support from Lurdes Martins, Vânia Sousa, and Paula Oliveira for their technical assistance.

Statement of Ethics

This study was conducted in accordance with Declaration of Helsinki and local Ethics Committee approval was obtained. Written informed consent was obtained from the patient for publication of this case report and any accompanying images.

Conflict of Interest Statement

The authors have no disclosures or other conflicts of interest to report.

Funding Sources

None of the authors has received grants for this submission.

Author Contributions

All the authors have contributed to this paper.

References

1 Remmer MH, Rastogi N, Ranka MP, Ceisler EJ. Achromatopsia: a review. Curr Opin Ophthalmol. 2015;26(5):333–40.
2 Hirji N, Aboshiha J, Georgiou M, Bainbridge J, Michaelides M. Achromatopsia: clinical features, molecular genetics animal models and therapeutic options. Ophthalmic Genet. 2018 Apr;39(2):149–57.
3 Katagiri S, Hayashi T, Yoshitake K, Sergeev Y, Akahori M, Furuno M, et al. Congenital achromatopsia and macular atrophy caused by a novel recessive PDE6C mutation (p.E591K). Ophthalmic Genet. 2015;36(2):137–44.
4 Aboshiha J, Dubis AM, Carroll J, Hardcastle AJ, Michaelides M. The cone dysfunction syndromes. Br J Ophthalmol. 2016;100(1):115–21.
5 Roosing S, Thiadens AA, Hoyng CB, Klaver CC, den Hollander AI, Cremers FP. Causes and consequences of inherited cone disorders. Prog Retin Eye Res. 2014;42:1–26.
6 Thiadens AA, Phan TM, Zekveld-Vroon RC, Leroy BP, Van Den Born LI, Hoyng CB, et al. Clinical course, genetic etiology, and visual outcome in cone and cone-rod dystrophy. Ophthalmology. 2012;119(4):819–26.
7 Michalakis S, Schön C, Becirovic E, Biel M. Gene therapy for achromatopsia. J Gene Med. 2017;19(3).
8 Georgiou M, Litts KM, Kalitzeos A, Langlo CS, Kane T, Singh N, et al. Adaptive optics retinal imaging in CNGA3-associated achromatopsia: retinal characterization, interocular symmetry, and intrafamilial variability. Investig Ophthalmol Vis Sci. 2019;60(1):383–96.
9 Tachibanaki S, Shimauchi-Matsukawa Y, Arinobu D, Kawamura S. Molecular mechanisms characterizing cone photoresponses. Photochem Photobiol. 2006;83(1):19–26.
10 Cote RH. Characteristics of Photoreceptor PDE (PDE6): similarities and differences to PDE5. Int J Impot Res. 2004;16 Suppl 1:S28–33.
11 Arshavsky VY, Lamb TD, Pugh EN. G proteins and phototransduction. Annu Rev Physiol. 2002;64(1):153–87.
12 Grau T, Artemyev NO, Rosenberg T, Dollfus H, Haugen OH, Cumhur Sener E, et al. Decreased catalytic activity and altered activation properties of PDE6C mutants associated with autosomal recessive achromatopsia. Hum Mol Genet. 2011;20(4):719–30.
13 Thiadens AA, den Hollander AI, Roosing S, Nabuurs SB, Zekveld-Vroon RC, Collin RW, et al. Homozygosity mapping reveals PDE6C mutations in patients with early-onset cone photoreceptor disorders. Am J Hum Genet. 2009;85(2):240–7.
14 Weisschuh N, Stingl K, Audo I, Biskup S, Bocquet B, Branham K, et al. Mutations in the gene PDE6C encoding the catalytic subunit of the cone photoreceptor phosphodiesterase in patients with achromatopsia. Hum Mutat. 2018;39(10):1366–71.
15 Georgiou M, Robson AG, Singh N, Pontikos N, Kane T, Hirji N, et al. Deep phenotyping of PDE6C-associated achromatopsia. Invest Ophthalmol Vis Sci. 2019;60(15):5112–23.
16 Robson AG, Nilsson J, Li S, Jalali S, Fulton AB, Tormene AP, et al. ISCEV guide to visual electrodiagnostic procedures. Doc Ophthalmol. 2018;136(1):1–26.
17 Crd AD. Cone-rod dystrophy sequencing panel with CNV detection. 2012;2.
18 Gopalakrishna KN, Boyd K, Artemyev NO. Mechanisms of mutant PDE6 proteins underlying retinal diseases. Cell Signal. 2017;37:74–80.
19 Cheguru P, Majumder A, Artemyev NO. Distinct patterns of compartmentalization and proteolytic stability of PDE6C mutants linked to achromatopsia. Mol Cell Neurosci. 2015;64:1–8.
20 Kohl S, Jägle H, Wissinger B, Zobor D. Achromatopsia summary genetic counseling GeneReview scope suggestive findings. 2019;1–25.
21 Huang L, Xiao X, Li S, Jia X, Wang P, Sun W, et al. Molecular genetics of cone-rod dystrophy in Chinese patients: new data from 61 probands and mutation overview of 163 probands. Exp Eye Res. 2016;146:252–8.
22 Greenberg JP, Sherman J, Zweifel SA, Chen RW, Duncker T, Kohl S, et al. Spectral-domain optical coherence tomography staging and autofluorescence imaging in achromatopsia. JAMA Ophthalmol. 2014;132(4):437–45.
23 Georgiou M, Robson AG, Singh N, Pontikos N, Kane T, Hirji N, et al. Deep phenotyping of PDE6C-associated achromatopsia. Invest Ophthalmol Vis Sci. 2019;60(15):5112–23.